We are IntechOpen, the world's leading publisher of Open Access books
Built by scientists, for scientists

6,900
Open access books available

186,000
International authors and editors

200M
Downloads

154
Countries delivered to

Our authors are among the

TOP 1%
most cited scientists

12.2%
Contributors from top 500 universities

Interested in publishing with us?
Contact book.department@intechopen.com

Numbers displayed above are based on latest data collected.
For more information visit www.intechopen.com

Nonlinear Optical Absorption of Organic Molecules for Applications in Optical Devices

Leonardo De Boni, Daniel S. Corrêa and Cleber R. Mendonça
Instituto de Física de São Carlos, Universidade de São Paulo
Brazil

1. Introduction

Nonlinear optical materials play a major role in the technology of photonics. To further advance the performance of optical devices, researchers have sought for materials with enhanced nonlinear optical properties, including inorganic semiconductors, polymeric systems and other organic molecules. The latter, specifically, are of great interest because they present high nonlinear optical properties combined with versatility of available routes of synthesis, used to alter and optimize molecular structure to maximize nonlinear responses and other properties. To select a material for a specific application, it is important to characterize its nonlinear optical absorption in a broad spectral range, in order to choose the optimized excitation wavelength. This book chapter describes resonant nonlinear optical absorption spectrum of the organic molecules Chlorophyll A, Indocyanine Green, Ytterbium Bisphthalocyanine and Cytochrome C, which are materials with potential applications in nonlinear optical devices. These organic molecules present distinct nonlinear optical absorption, such as saturable absorption (SA) and reverse saturable absorption (RSA), depending on the laser excitation wavelength and pulse duration. In order to investigate the excited state absorption and the population dynamics of the molecules, two distinct Z-scan methodologies were used, both based on measurements of the sample's transmittance under laser excitation. The main difference between the methods employed is the possibility to monitor nonlinear effects in distinct temporal regimes, and then observe effects related with singlet and triplet electronic transitions, which, in most cases, can only be discriminated by the temporal dynamic of the system. While one technique uses a sequence of picoseconds pulses to induce and probe nonlinear absorption dynamics between singlet and triplet states, the other one employs femtosecond white-light supercontinuum pulses to map the spectrum of the excited state absorption in the visible and near infrared. By using both methods, one can determine and quantify nonlinear effects from femtoseconds up to hundreds of nanoseconds, including singlet excited state absorption cross-section spectrum and other spectroscopic features, such as decaying time (ranging from femtoseconds to a few nanoseconds) and triplet excited state cross-section. Once one is able to temporally and spectrally map the nonlinearity of materials, it can be predicted how a given nonlinear optical device will act in distinct regimes (temporal, spectral and of intensity). Specifically, Chlorophyll A and Ytterbium Bisphthalocyanine present large RSA or SA depending on the excitation wavelength. Indocyanine Green presents high singlet and triplet excited state absorptions. Cytochrome C also presents saturable absorption, with short singlet-state

lifetime and a relatively fast intersystem-crossing time. Therefore, information on the temporal dynamics combined with the excited state absorption cross-section and intensity regime can guide the development of applications based on the organic molecules presented here. Some notable applications of these materials in optical devices include all-optical switches, nonlinear optical limiters, and also bio-related applications, such as Photodynamic Therapy (PDT).

2. Nonlinear optics

Nonlinear optics processes are responsible for the nonlinearity of materials, phenomena which include nonlinear absorption, nonlinear refraction, and induced scattering, among others. The origin of such nonlinearities varies considerably. For instance, nonlinear absorption may be related to two-photon absorption, excited state absorption and free-carrier absorption. There are good reviews in the literature about two-photon absorption (He et al., 2008, Prasad, 1991) and free-carrier absorption (Banfi et al., 1998, He et al., 2008). This chapter will specifically focus on excited state absorption.

Classification of optical nonlinearities usually falls in two main categories: instantaneous and accumulative (slow) nonlinearities. In the instantaneous case, the instantaneous polarization induced by the applied electromagnetic field in the medium can be expressed by an expansion in a Taylor series of the electric field amplitude, according to (Shen, 1984):

$$\vec{P} = \chi^{(1)} \cdot \vec{E} + \chi^{(2)} \cdot \vec{E}\vec{E} + \chi^{(3)} \cdot \vec{E}\vec{E}\vec{E} \tag{1}$$

In Eq. (1), the quadratic term with the electric field describes the first nonlinear effect. The coefficient $\chi^{(2)}$ is named complex susceptibility tensor of order 2. Its magnitude describes the intensity of the 2nd order nonlinear effect, which, in turn, is related to second harmonic generation, optical rectification and sum and difference frequency mixing. Such effects are only observed in noncentrosymmetric materials.

The coefficient $\chi^{(3)}$ is named complex susceptibility tensor of order 3 and describes the intensity of the 3rd order nonlinear effect, such as self-focusing action, third harmonic generation and two-photon absorption. Materials presenting non-zero $\chi^{(3)}$ (e.g., materials exhibiting two-photon absorption) are candidates as active medium for several technological applications, for which there are good reviews available in literature (Bhawalkar et al., 1996, He et al., 2008, Prasad & Willians,1991). However, such materials are out of the scope of this book chapter, which will describe organic molecules' nonlinear effects arising only from resonant absorption. In the case of resonant absorption, the accumulative nonlinearities may occur in a time scale longer than the pulse duration. For instance, the polarization density generated by an applied field may develop or decay in a time scale longer than the excitation duration. Such interactions are normally dissipative, causing energy transfer from the absorbed field to the medium, which triggers the nonlinearity. Therefore, on the contrary to instantaneous nonlinearity, accumulative nonlinearities are strictly dependent on the amount of energy stored into the medium. Examples of such accumulative nonlinearities include resonant excited state absorption, such as saturation of absorption (SA) and reverse saturable absorption (RSA), which find applications in the construction of nonlinear optical devices.

2.1 Nonlinear effects arising from excited states

Nonlinear optical effects can also be associated to one-photon absorption (resonant) processes when they cause significant population change of the material's electronic states. When a medium is excited to a higher energy level, the linear polarization of material, $\vec{P} = \chi^{(1)} \cdot \vec{E}$, cannot be held constant. In this case, let us consider a simplified picture of a medium possessing two energy levels (ground and excited states), so that $\chi = n_g \chi_g + n_e \chi_e$, in which χ_g and χ_e represent the electrical susceptibilities of ground and excited state respectively. The linear electrical susceptibility of excited molecules is other than that in the ground state and can be expressed as $\chi = \chi_g + n_e(\chi_e - \chi_g)$, where $n_g + n_e = 1$. The term n_e describes the population fraction lying in the excited state (N_e / N_0), in which $N_0 = N_g + N_e$ is the total number of molecules of the system, and N_e and N_g are the excited and ground state population, respectively. This description of polarization is not linear with the electric field anymore, because the excited state population fraction depends on the light intensity, which is equivalent to the square of the electric field, according to (Pang et al.,1991):

$$\vec{P} = \chi_g^{(1)} \cdot \vec{E} + \frac{N_e}{N_0}(\chi_e^{(1)} - \chi_g^{(1)}) \cdot \vec{E} \tag{2}$$

The second term of Eq. (2) presents a nonlinear relation to the electric field and depends on the linear susceptibility of the ground and excited states. Therefore, the nonlinear susceptibility in Eq. (1) presents resonant terms that are dependent on the population fraction of molecules. Considering a case of a centro-symmetric material (all even susceptibilities are null), the nonlinear polarization can be rewritten as:

$$\vec{P} = \chi_g^{(1)} \cdot \vec{E} + \chi_g^{(3)} : \vec{E}\vec{E}\vec{E} + \frac{N_e}{N_0}(\chi_e^{(1)} - \chi_g^{(1)}) \cdot \vec{E} + ... \tag{3}$$

This new polarization contains resonant and non-resonant effects induced by the electric field of a laser beam. The evolution of the nonlinear effect related to the population of excited states can be monitored by rate equations that describe every electronic transition involved in the absorption. The temporal population evolution of a given excited state can be described by (Pang et al.,1991):

$$\frac{dn_e(t)}{dt} = -\frac{n_e(t)}{\tau} + (1 - n_e(t))\frac{\sigma(\nu)I}{h\nu} \tag{4}$$

in which $\sigma(\nu)$ is the one-photon absorption cross-section, $h\nu$ is the photon energy, and τ is the excited state relaxation time. $\sigma(\nu)I/h\nu$ describes the molecules transition from the ground to the excited state. The solution to this equation is given by:

$$n_e(t) = \frac{\sigma(\nu)}{h\nu}e^{-t/\tau}\int_{-\infty}^{t} I(t')e^{t/\tau'}dt' \tag{5}$$

This integral contains the light intensity I and τ', defined as $\tau' = \tau/(1 + I/I_{sat})$, where $I_{sat} = h\nu/\sigma\tau$ is the saturation intensity of the medium, which occurs as the lowest energy state is depopulated. The temporal evolution of the population from each state provides a

dynamic absorption coefficient to the material. For instance, for a material that possesses two excited states, the absorption coefficient can be defined as $\alpha(t) = N_0(n_0(t)\sigma_{01} + n_1(t)\sigma_{12})$, in which σ_{01} and σ_{12} are the one-photon absorption cross-sections related to absorption from the ground to the first excited state, and from the first excited state to the second one, respectively.

3. Applications in nonlinear optical devices

The integration of all-optical and electro-optical devices into the current technology has led to the development of a large number of schemes for controlling and manipulating the phase, direction, polarization and amplitude of optical beams. The ability to control light intensity is of prime relevance in optical-related applications, such as optical communications, optical computing and light-driven chemical reactions. The methods to control the amplitude of light can be generally divided into two major groups: dynamic and passive methods. The first method is accomplished by a device that receives an external feedback, such as an iris or a power optical filter to control the light intensity incident on an optical system. Such method requires other devices to work along in the acquisition (*e.g.*, a sensor, a processor, etc), leaving the process slower and more complex. On the other hand, passive control is obtained by using a nonlinear optical material, in which sensing, processing and actuation are inherent, making the devices simpler and faster. Within the classification of passive devices to control the amplitude of an optical signal, two of great importance are all-optical switches and optical limiters. An ideal optical switch is a nonlinear optical device that is activated at a specific intensity or fluence threshold, becoming totally opaque. In contrast, an ideal optical limiter is a device that exhibits a linear transmittance below a specific intensity or fluence level but, above this level, its output intensity becomes constant. Optical limiters have been used in several applications, such as passive mode locking, pulse compression, and the most popular application: eye and sensor protection in optical system (*e.g.*, telescopes and night vision systems).

For instance, one can construct optical limiters with responses that are insensitive to the incident pulse duration. The resonant nature of the accumulative nonlinearities (such as SA and RSA), however, frequently results in a narrow bandwidth of operation for devices utilizing these mechanisms. By contrast, optical limiters that rely on instantaneous (nonresonant) nonlinearities can be broad band. These nonlinearities, however, require high intensities and typically operate effectively only for very short optical pulses. Therefore, by using an appropriate optical limiter in terms of nature and threshold value, one can extend the lifetime of a device and allow it to continue to operate under severe conditions.

4. Techniques employed to determine the materials' nonlinear optical properties

4.1 Z-scan technique in the nano- and picosecond regime

In order to characterize the nonlinear optical absorption of organic molecules in the nano- and picosecond regime, the open aperture Z-scan technique, developed originally by Sheik-Bahae et. al. (Sheik-Bahae et al.,1989), can be used. Basically, this technique monitors the change in the nonlinear transmittance as the sample is scanned through the Z-axis, which contains a focused Gaussian laser beam. An extension of this technique, called Z-scan

technique with pulse train (Misoguti et al.,1999), can also be employed, allowing the investigation of the time evolution of nonlinear processes. The excitation source is a frequency-doubled, Q-switched and mode-locked Nd:YAG laser, delivering pulses at 532 nm and 100 ps. Each pulse train contains about 20 pulses separated by 13 ns at a 10 Hz repetition rate. This low repetition rate is generally used to avoid cumulative thermal nonlinearities. The beam is focused onto a quartz cell, yielding diameters of tens of μm at the focal plane. A photodetector placed in the far field coupled with a digital oscilloscope and a computer are used to acquire the pulse train signal. Each peak height is proportional to the corresponding pulse fluence, once the detection system has a rise time slower than the 100 ps pulse duration. By measuring the beam waist and the pulse train average power, one can find out the pulse fluency. The intensity can be determined by carrying out Z-scan measurements with CS_2. When the sample is located at the focus, the pulse train signal is acquired. Then, this signal is normalized to the one obtained when the sample is far from the focus, yielding the normalized transmittance as a function of pulse number. All optical measurements were carried out with the sample placed in a quartz cuvette. Figure 1 schematically shows the experimental setup.
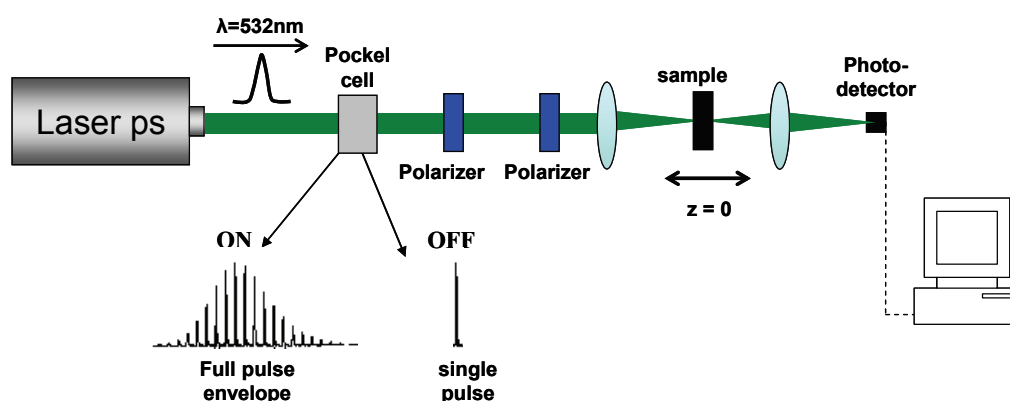

Fig. 1. Experimental setup of the Z-scan technique with pulse trains, used to characterize the material's nonlinear response in the pico- and nanosecond regime.

4.2 Z-scan technique in the femtosecond regime

The nonlinear optical absorption of organic molecules in the femtoseconds regime in a large spectral range may be carried out by means of two methodologies: (a) Single wavelength Z-scan technique and (b) White-Light Continuum Z-scan technique, described in more details as follows.

(a) Single wavelength Z-scan technique

This methodology uses a Ti:sapphire chirped pulse laser amplified system that produces pulses of 150 fs centered in 775 nm, with a repetition rate of 1 kHz, to pump an optical parametric amplifier (OPA), which, in turn, generates wavelengths in the spectral region from 460 nm to 2200nm of nearly 100 fs. Figure 2 (a) schematically displays the details of the Single wavelength Z-scan technique experimental setup.

(b) White-Light Continuum (WLC) Z-scan technique

In this methodology, whose full details can be found elsewhere,(Balu et al., 2004, De Boni et al., 2004), the White-light Continuum (WLC) is produced by focusing a femtoseconds laser

beam (Ti:sapphire chirped pulse laser amplified system that produces 150 fs centred in 775 nm, with a repetition rate of 1 kHz,) with a lens onto a quartz cell containing distilled water. A low-pass filter is used to remove the strong pump pulse and the infrared part of the WLC spectrum. The use of typically 0.3 mJ laser pulses generates about 10 µJ of WLC, spanning from 420 up to 750 nm. After re-collimation, the WLC beam is focused onto the sample, which is scanned along the beam propagation z-direction, as usually done in the traditional Z-scan method. The WLC transmitted through the sample is completely focused onto a portable spectrometer with a resolution of ~1 nm. The spectra are acquired for each z position as the sample is scanned along the z-direction and then normalized to the one obtained far from the focal plane. By selecting a particular wavelength from the complete set of measured spectra, a Z-scan signature is obtained according to the nonlinear response at that wavelength. Figure 2 (b) schematically shows the experimental apparatus of the WLC Z-scan technique. When using this technique under resonant conditions, the white-light continuum pulse chirp must be considered, since distinct spectral components will reach the sample at distinct times. Consequently, cumulative effects can occur as result of absorption by excited molecules, which are then promoted to a higher excited state.
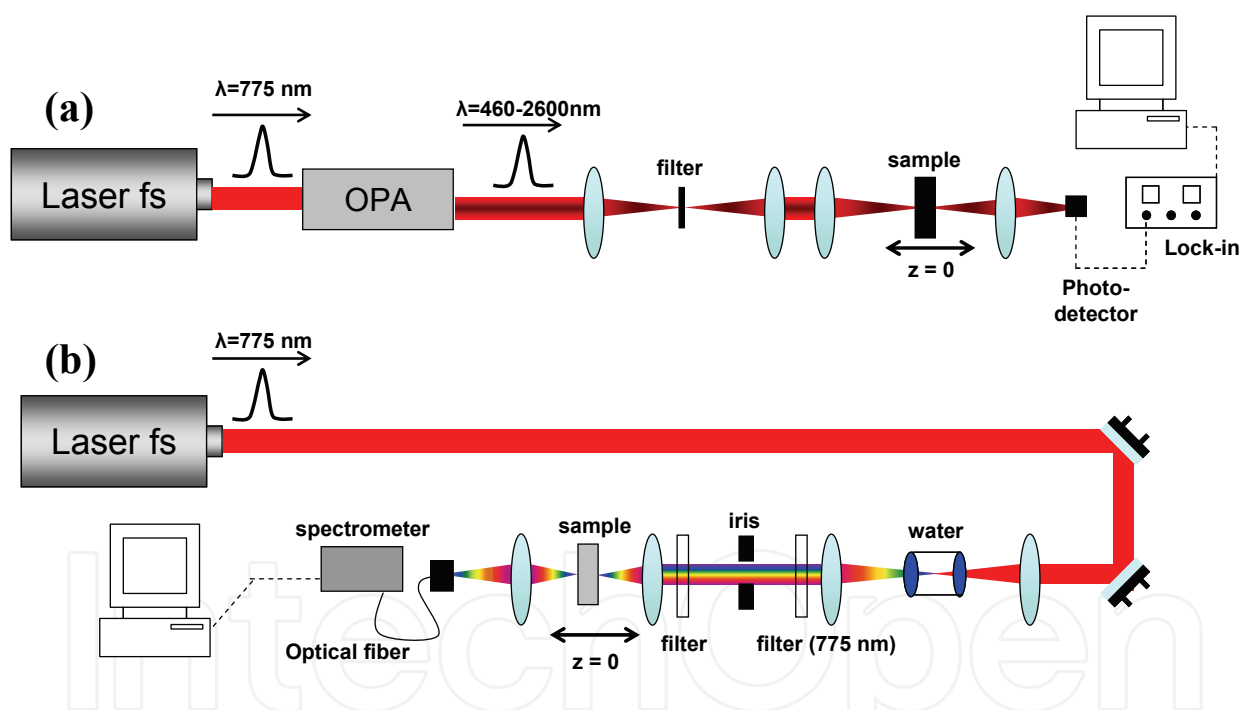

Fig. 2. Experimental setup of the (a) Single wavelength and (b) WLC Z-scan techniques, used to characterize the material's nonlinear response in the femtosecond regime.

5. Nonlinear optical absorption (NLOA) of organic molecules

In this section, the results of the nonlinear optical absorption (NLOA) of the molecules Chlorophyll A, Indocyanine Green, Ytterbium Bisphthalocyanine and Cytochrome C are presented. The molecules are characterized in the nano, pico and femtoseconds regimes and present Reverse Saturable Absorption (RSA) and Saturable Absorption (SA), with potential applications in nonlinear optical devices.

5.1 Chlorophyll A
5.1 (a) NLOA in the nano and picosecond regimes

Chlorophyll A, belonging to the class of porphyrins, is a biomolecule of prime importance in the photophysical processes of plants, acting in the conversion of light into chemical energy in several biological systems (Michel-Beyerle, 1985, Scheidt & Reed, 1981) by taking part in the light absorption and electron transfer in the photosynthetic reaction center (Baker & Rosenqvist, 2004, Carter & Spiering, 2002, Michel-Beyerle, 1985). Due to its relevance in biological processes, Chlorophyll A has been the subject of extensive theoretical and experimental studies (Gouterman, 1961, Hasegawa et al., 1998, Parusel & Grimme, 2000, Sundholm, 1999). Furthermore, porphyrins have been proposed for medical and photonics applications such as optical limiters (Calvete et al., 2004, Neto et al., 2003, Neto et al., 2006, O'Flaherty et al., 2003), optical switches (Loppacher et al.,2003), and sensitizers for photodynamic therapy (Fisher et al.,1995). Hence, studying Chlorophyll A excited states properties is essential to understand biological processes aiming at possible applications in photonics and medicine.

The electronic transitions of Chlorophyll A are usually characterized by two regions: the Q-band, which is relatively weak and occurs in the visible region; and the intense Soret or B-band, which appears in the near UV region and is often accompanied by an N-band of lower intensity (see Figure 3). The linear absorption spectrum of Chlorophyll A has been understood in terms of the four-orbital model applied by Gouterman (Gouterman, 1961), which although very simple reproduces all the major features of this system. There are several theoretical studies carried out using distinct methods to further understand the electronic excited states of Chlorophyll A (Hasegawa et al., 1998, Parusel & Grimme, 2000, Sundholm, 1999). In general, these works assign more than one electronic excited state to describe the experimentally observed features of Chlorophyll A spectrum (Q and B-band). In this book chapter, the choice was based on the electronic states reported by Parusel *et al.* (Parusel & Grimme,2000) obtained through the DFT/MRCI method (density functional theory and multireference configuration interaction), which gives the best interpretation for the linear absorption spectrum of Chlorophyll A, as the basis for the energy diagram employed here to understand the results. The Q-band at 670 nm is the main transition
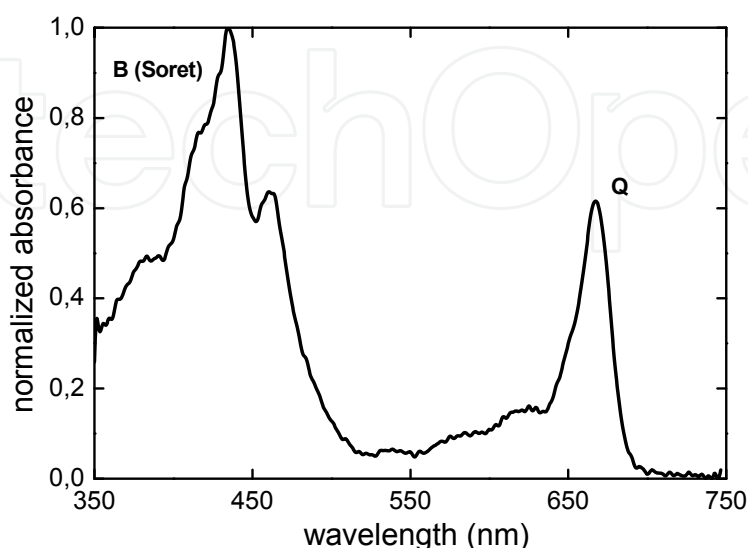

Fig. 3. Absorption spectrum of Chlorophyll A/chloroform solution.

excited by the 532 nm light used in this investigation. This molecule has considerable absorption in the 600-700 nm region, in which human tissues are more transparent. In terms of medical therapy, for instance, light can reach the dye molecule adsorbed in the cells and undergo a photoreaction, i.e. Chlorophyll A satisfies an important requirement for possible use as a sensitizer in PDT.

The emission spectrum at room temperature for excitation at the Q-band presents a strong fluorescence peak at 669 nm, which means that the Q-band is the predominant excitation path. The fluorescence lifetime (τ_f) reported in the literature is 4 ns (Vernon & Seely, 1996).

Based on the absorption and emission spectra and on models traditionally used for other porphyrins, a simplified five-level energy diagram can be sufficient to describe the dynamics of the nonlinear absorption in the picosecond regime, as illustrated in Figure 4.
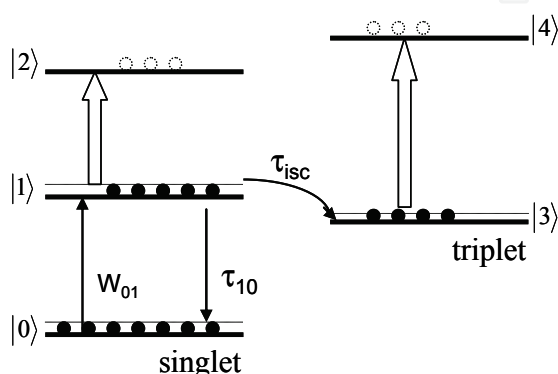

Fig. 4. Five-level energy diagram used to simulate the experimental results.

Figure 5 shows experimental results (open circles) for the nonlinear absorption obtained with the Z-scan technique with pulse train at 532 nm (Correa et al., 2002) and theoretical fitting (solid line) using the five-level energy diagram depicted in Figure 4. The strongest peak in the pulse train was arbitrarily labeled "0." The irradiance is $I_{(0)}$ = 0.35 GW/cm².

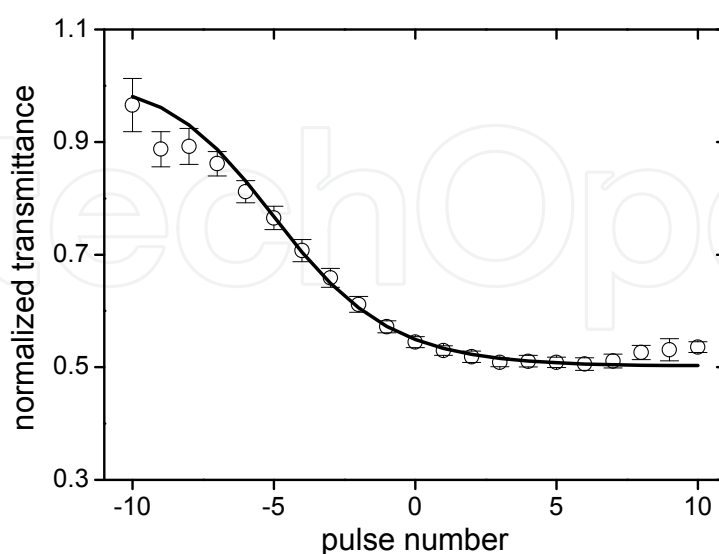Fig. 5. Normalized transmittance of Chlorophyll A/chloroform solution along the pulse train for a $I_{(0)}$ =0.35 GW/cm². Solid line is the theoretical curve obtained by using the five-level energy diagram.

To understand the changes in the nonlinear effect during the train of pulses, basically, one needs to comprehend how the population dynamic is produced by the pulse train. When the first pulse of the pulse train is absorbed by the sample, it will promote molecules from the ground state $|0\rangle$ to the excited singlet state $|1\rangle$. The fraction of population on the singlet excited state $|1\rangle$ may decay radiatively to level $|0\rangle$, with the characteristic lifetime of the state (τ_{10}), or relax to an excited triplet state $|3\rangle$, with the lifetime τ_{isc}, known as intersystem-crossing time. Also, because the lifetimes involved in this nonlinear process have the same order of the time between two consecutives pulses (13 ns), molecules already in $|1\rangle$ and $|3\rangle$ do not have enough time to completely relax back to the ground singlet state. Based on this fact, the next pulse of the pulse train will probe a different population in the electronic states than the first pulse did. If the absorption cross-sections are different, the transmittance of such pulse will be proportional to the new absorption coefficient. This mechanism will be present to the other pulses, as an accumulative effect. In addition, because the higher excited states, $|2\rangle$ and $|4\rangle$, are short-lived, their populations can be neglected. On the basis of this energy diagram, the set of rate equations that describe the fraction of molecules (n_i) at each level is:

$$\frac{dn_0}{dt} = -n_0 W_{01} + n_1 \left(\frac{1}{\tau_f} - \frac{1}{\tau_{isc}} \right) \tag{6}$$

$$\frac{dn_1}{dt} = n_0 W_{01} - \frac{n_1}{\tau_f} \tag{7}$$

$$\frac{dn_3}{dt} = \frac{n_1}{\tau_{isc}} \tag{8}$$

where $W_{01} = \sigma_{01} I / h\nu$ is the transition rate. This set of equations was numerically solved using the actual temporal intensity pattern of the Q-switched/mode-locked pulse train of our experiment, yielding the population dynamics, $n_i(t)$. The time evolution of the nonlinear absorption can be calculated according to:

$$\alpha(t) = N\{n_0 \sigma_{01} + n_1 \sigma_{12} + n_3 \sigma_{34}\} \tag{9}$$

where N is the sample concentration, and σ_{12} and σ_{34} are the excited state cross-sections. The ground state cross-section, σ_{01}, was determined by measuring the linear absorption at 532 nm ($\alpha = N\sigma_{01}$). This procedure resulted in $\sigma_{01} = 3.1 \times 10^{-18}$ cm². The numerical calculation was carried out with $\tau_f = 4$ ns. In Figure 5, the solid line represents the theoretical fittings obtained with $\sigma_{12} = 4 \times 10^{-18}$ cm², $\sigma_{34} = 8 \times 10^{-18}$ cm², and $\tau_{isc} = 1.5$ ns. The absorption cross-section of the triplet state is higher than that of the singlet, although with a low ratio (only 2 times). On the other hand, the intersystem-crossing lifetime (1.5 ns) is shorter than the typical values reported for porphyrins and phthalocyanines.(Frackowiak et al., 2001, Shirk et al., 1992). This short intersystem-crossing lifetime indicates an efficient singlet-triplet conversion, which makes Chlorophyll A suitable for applications as a PDT sensitizer. This efficient intersystem-crossing (singlet-triplet) conversion is consistent with

those found for Mg phthalocyanine, which has a yield of triplet formation higher than for most phthalocyanines.(Frackowiak et al., 2001)

5.1 (b) NLOA in the femtosecond regime

This section presents the study of the excited state absorption of Chlorophyll A in the femtosecond regime by measuring its nonlinear absorption spectrum from 460 nm to 700 nm using the WLC Z-scan technique. Its resonant nonlinear absorption spectrum presents saturable absorption (SA) and reverse saturable absorption (RSA) depending on the excitation wavelength (De Boni et al., 2007). Figure 6 displays Z-scan curves of Chlorophyll A for some pump wavelengths of the WLC spectrum. An inversion of the normalized transmittance is observed as the nonlinear process changes from RSA (shorter wavelengths) to SA (longer wavelengths).
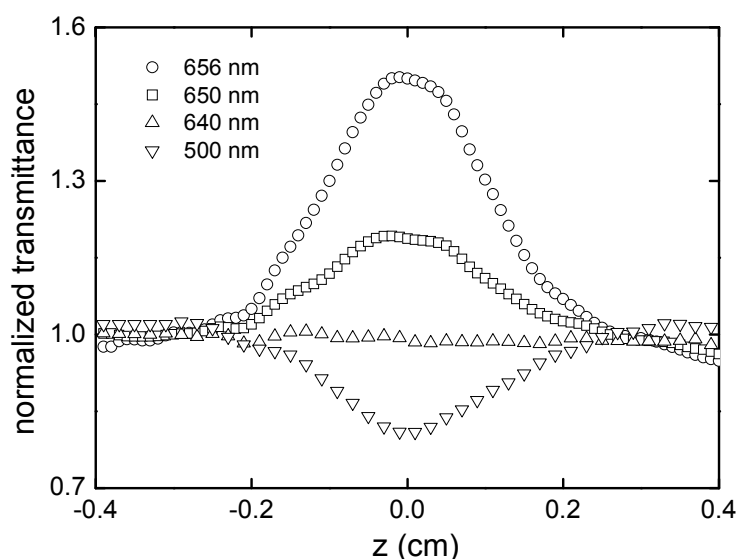

Fig. 6. Experimental Z-scan curves for Chlorophyll A obtained with the WLC Z-scan technique. An inversion of the normalized transmittance is observed according to the dominant nonlinear process (SA or RSA).

Because the white-light continuum pulse temporal width is around 5 ps, only the singlet levels of Figure 4 were used to establish the population dynamics of Chlorophyll A. In this case, molecules in the ground state $|0\rangle$ can be promoted to the first excited state $|1\rangle$ (Q-band) by one-photon absorption, being subsequently excited to a higher excited level. This level does not correspond to the B-band (Linnanto & Korppi-Tommola, 2000, Rivadossi et al., 2004, Wehling & Walla, 2005, Zigmantas et al., 2002) but to a distinct electronic state in the UV region, since the photons used to transition an electron from $|1\rangle$ to a higher excited state belong to the blue spectral region of the WLC pulse and, therefore, are more energetic than those required to promote a transition from $|1\rangle$ to the B-band. The relaxation from level $|1\rangle$ to the ground state can be neglected because of the short pulse temporal width of the WLC pulse. The upper energy levels (located above $|1\rangle$) are assumed to be too short-lived and, therefore, present no appreciable population (Shank et al.,1977). As a consequence, molecules are accumulated only in the first excited state and the absorption cross-section between states $|1\rangle$ and upper energy levels (located in the UV region) can be determined. In

this case, no triplet state was considered, since the intersystem-crossing time of Chlorophyll A is in the order of nanoseconds (Correa et al.,2002), which is much longer than the duration of the WLC pulse used. Based on these considerations, the rate equation used to describe the dynamic change of absorption, in accordance with the energy-level diagram, is:

$$\frac{dn_0(t)}{dt} = -n_0(t)W_{01}(\lambda) + \frac{1-n_0(t)}{\tau_{10}} \tag{10},$$

in which $n_1(t) = 1 - n_0(t)$ and $W_{01}(\lambda) = \sigma_{01}(\lambda)I/h\nu$ is the transition rate, where $\sigma_{01}(\lambda)$ is the ground state cross-section. I is the excitation intensity, $n_i(t)$ is the population fraction in each state, h is the Planck constant, and ν is the photon frequency. Due to the WLC pulse chirp, its red portion (resonant with the Q-band) promotes part of the population to the first excited state $|1\rangle$ and consequently the other spectral components of the WLC pulse probe the excited state absorption (ESA), once the first excite state has a lifetime longer than the pulse duration. The time evolution of the nonlinear absorption, $\alpha(\lambda,t)$, was calculated according to:

$$\alpha(\lambda,t) = N[n_0(t)\sigma_{01}(\lambda) + n_1(t)\sigma_e(\lambda)] \tag{11},$$

where N is the number of molecules/cm³ and $\sigma_e(\lambda)$ is the excited state cross-section correspondent to the transition $|1\rangle$ to a higher excited state. The first and the second terms in Eq. (11) provide the absorption coefficient of the ground and excited states respectively. Since the ground state absorption cross-section for every spectral component is determined through the linear absorption spectrum, the only adjustable parameters are the excited state cross-sections. By fitting the normalized transmittance spectrum, it is possible to determine the excited state cross-sections of Chlorophyll A for each wavelength within the WLC spectrum. These values are displayed in Figure 7 (closed triangles). The region below 450 nm was omitted because the white-light spectrum generated in the experiment starts around this wavelength. The difference between the values of ground and excited state cross-sections ($\sigma_{01} - \sigma_e$) is also displayed in Figure 7 (open triangles). From these data, one can observe the singlet excited state processes of Chlorophyll A. When $\sigma_{01} - \sigma_e > 0$, there is a decrease in the total absorption coefficient, α, characterizing SA. For Chlorophyll A, this process was observed from 700 nm up to 640 nm. Around 635 nm, the values of σ_{01} and σ_e are the same, giving rise to no appreciable change in the normalized transmittance at this wavelength.

It can be observed that σ_e values (closed triangles) are zero from 700 nm up to 665 nm, indicating that, for this range, there is no transition to a higher excited state. The red portion of the WLC, which is resonant with the Q-band, causes ground state depletion, responsible for the SA. Therefore, up to 665 nm, the WLC is populating state $|1\rangle$, which is then probed by the remaining components of WLC pulse. Consequently, for wavelengths shorter than 665 nm, the values of σ_e are not zero, due to the transition from $|1\rangle$ to the higher excited state, which is allowed according to DFT/MRCI calculations presented in the literature (Parusel & Grimme, 2000). If $\sigma_{01} - \sigma_e < 0$, the material has its absorption coefficient increased with the intensity (RSA process), as shown by open triangles in Figure 7 for wavelengths below 640 nm. The excited state population build-up generated with the WLC Z-scan

technique can be advantageously used to shape the pulse intensity spectrum in order to match the most intense linear absorption band of the material. As a consequence, it is possible to obtain an enhancement of the nonlinear absorption in a transparent region through excited state absorption. In practical terms, WLC pulses could be used in applications where a high RSA process is needed in the blue region of the spectrum.
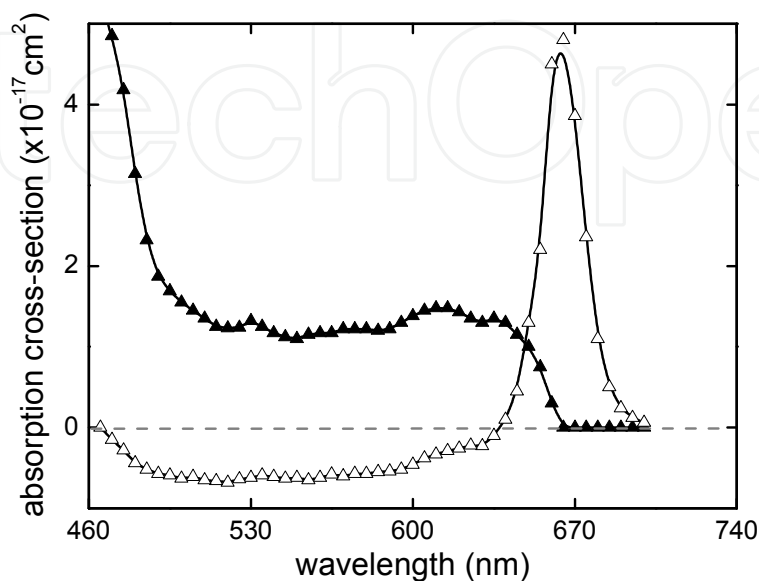
Fig. 7. Excited state (σ_e: closed triangles) cross-sections as a function of the excitation wavelength for Chlorophyll A obtained with the WLC Z-scan technique. The difference between the excited and ground state cross-section ($\sigma_{01} - \sigma_e$: open triangles) is also displayed.

5.2 Ytterbium Bisphytallocyanine
5.2 (a) NLOA in the nano and picosecond regimes

Phthalocyanines are planar organic molecules that can exhibit large third-order susceptibilities due to their high π-conjugation. To further increase the conjugation, and consequently enhance the nonlinear optical properties, one can augment the molecular size by adding peripheral rings or constructing sandwich compounds, known as Bisphthalocyanines ($YbPc_2$), where two phthalocyanine rings are coordinated to a central metal ion. Owing to their excellent environmental stability and optical properties, that can be tuned by varying the central metal ion, or a peripheral side-group, phthalocyanines and bisphthalocyanines are promising for manufacturing optical devices, such as optical-limiting devices. The basic principle of optical-limiting devices is the reverse saturable absorption (RSA), which is normally caused by an efficient intersystem-crossing process from a higher excited singlet state to an excited triplet state, competing with direct radiative decay to the singlet ground-state. This section reports on the dynamic optical nonlinearities of Ytterbium Bisphthalocyanine ($YbPc_2$)/chloroform solution obtained with the Z-scan technique with pulse trains. The dependence of the nonlinear absorption on the pulse fluence presents first SA, and subsequently RSA behavior. A six-energy-level diagram is used to establish the population dynamics and the mechanisms that contribute to the nonlinear refraction and absorption. (Mendonça et al., 2000)

Figure 8 shows that the absorption spectrum of YbPc$_2$ in chloroform solution is similar to those reported in the literature for other phytallocyanines containing metal-ions, and agrees with the energy-level diagram, shown in the inset, obtained from the valence-effective Hamiltonian (VEH) calculation.
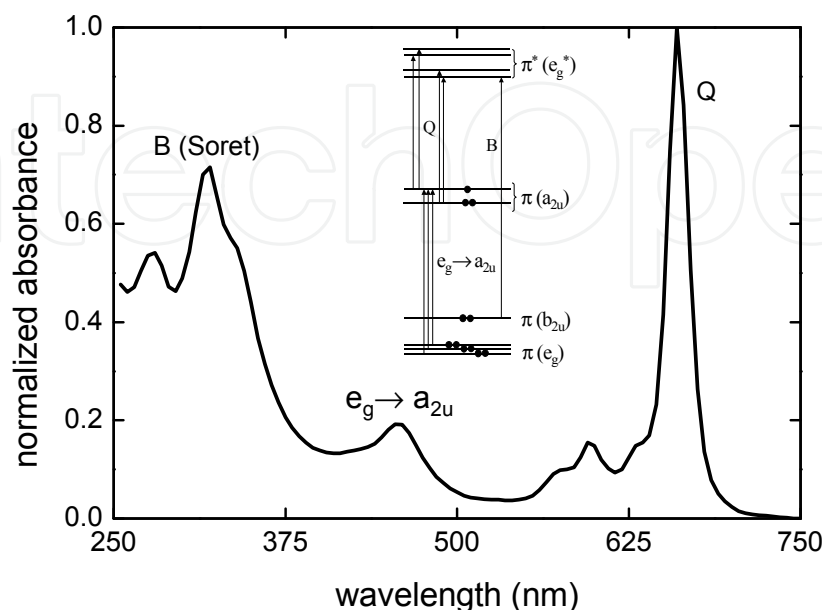

Fig. 8. Absorbance spectrum of YbPc$_2$ /chloroform solution. The inset depicts VEH one-electron energies of the molecular p-orbitals.

The structure around 650 nm, known as Q-band, is attributed to transitions from the split $\pi(a_{2u})$ orbital to the upper $\pi^*(e_g^*)$ orbital. The band around 460 nm corresponds to transitions from the deeper $\pi(e_g)$ level to the half occupied $\pi(a_{2u})$ orbital, while the B (Soret) band, which appears in the ultraviolet region (320 nm), is attributed to the transitions between $\pi(b_{2u})$ and $\pi^*(e_g^*)$ levels. According to the absorption spectrum, both the Q-band and the $e_g \to a_{2u}$ transition can, at first, be excited when 532 nm is employed. However, time-resolved fluorescence measurements for a pump at this wavelength resulted mostly in an emission centered on 550 nm, with a 4 ns lifetime, indicating that the $e_g \to a_{2u}$ transition is the main excitation path. A weaker 5 ns lifetime fluorescence (about 15% of the total) centered around 692 nm (Q-band) was also observed, indicating a secondary path for the excitation mechanism.

Figure 9 shows experimental results for the nonlinear absorption obtained with pulse trains Z-scan technique. To explain these results, the six-energy-level diagram depicted in Figure 10 is considered, which is a simplification of the one shown in the inset of Figure 8. Two possible ground state levels can be considered, $|0\rangle$ and $|1\rangle$, because two distinct bands ($a_{2u} \to e_g^*$ and $e_g \to a_{2u}$) can absorb photons of the excitation employed. According to the present model, molecules in state $|0\rangle$ can be promoted to level $|1\rangle$, when pumped by excitation at 532 nm, while molecules at level $|1\rangle$ can be excited to level $|2\rangle$. A two-photon absorption process ($e_g \to e_g^*$) could also be considered, but it was found to have little influence on the theoretical fitting. On the other hand, molecules excited to level $|1\rangle$ can decay radiatively to level $|0\rangle$, and those excited to level $|2\rangle$ can either decay radiatively to level $|1\rangle$ or undergo an intersystem-crossing to the triplet state $|4\rangle$. The upper excited singlet

and triplet levels, $|3\rangle$ and $|5\rangle$ respectively, are assumed to be too short-lived to present any significant population build up.
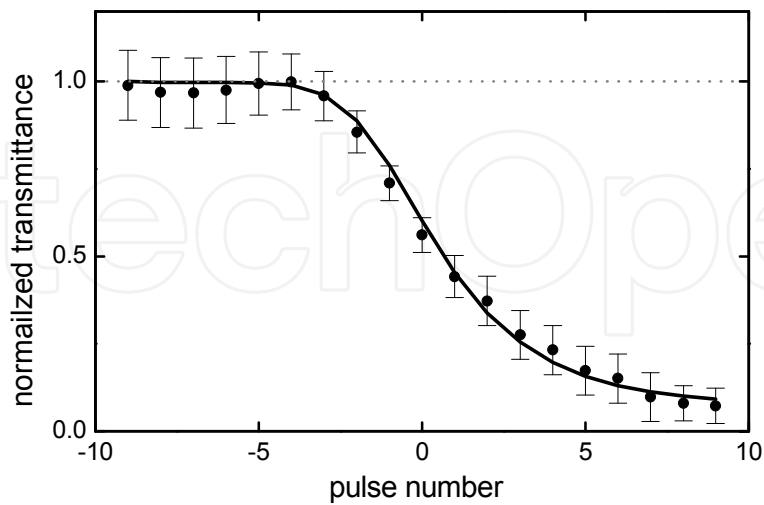

Fig. 9. Nonlinear absorption of YbPc$_2$ along the pulse train. Solid line is the theoretical curve obtained by using the six-energy-level diagram.
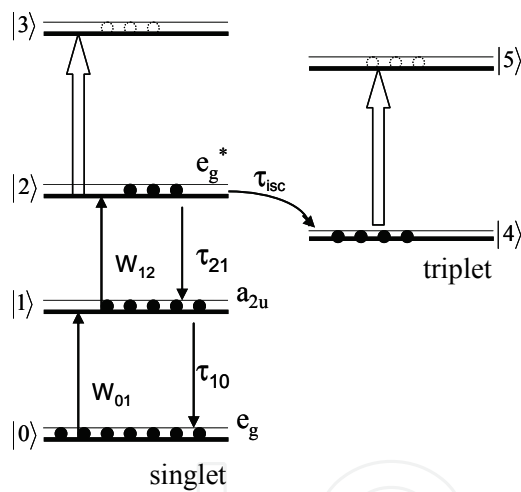

Fig. 10. Six-energy-level diagram used to simulate the experimental result of Ytterbium Bisphytallocyanine.

The rate equations used to describe the fractions of molecules, n_i, at each energy level are:

$$\frac{dn_0}{dt} = -n_0 W_{01} + \frac{n_1}{\tau_{10}}$$ (12)

$$\frac{dn_1}{dt} = n_0 W_{01} - n_1 W_{12} + \frac{n_2}{\tau_{21}} - \frac{n_1}{\tau_{10}}$$ (13)

$$\frac{dn_2}{dt} = n_1 W_{12} - \frac{n_2}{\tau_{21}} - \frac{n_2}{\tau_{isc}}$$ (14)

$$\frac{dn_4}{dt} = \frac{n_2}{\tau_{isc}} \tag{15}$$

where $W_{01} = \sigma_{01}I/h\upsilon$ and $W_{12} = \sigma_{12}I/h\upsilon$ are the transition rates, with σ_{01} and σ_{12} being the ground and excited state cross-sections, respectively. τ_{10} and τ_{21} are the lifetimes of levels $|1\rangle$ and $|2\rangle$, and τ_{isc} is the intersystem-crossing time. This set of equations was numerically solved using the actual temporal intensity pattern of the Q-switched and mode-lock pulse train of the experiment, yielding the population dynamics, $n_i(t)$. The time evolution of the nonlinear absorption can be calculated according to:

$$\alpha(t) = N\{n_0\sigma_{01} + n_1\sigma_{12} + n_2\sigma_{23} + n_4\sigma_{45}\} \tag{16}$$

where N is the concentration, and σ_{23} and σ_{45} are the excited state cross-sections. The excited state cross-sections, σ_{01}, determined by measuring the linear absorption at 532 nm, resulted in $\sigma_{01} = 2.4 \times 10^{-18} cm^2$. The numerical calculation was carried out with $\tau_{10} = 4$ ns and $\tau_{21} = 5$ ns, values obtained through time-resolved fluorescence measurements. The solid line in Figure 9 represents the theoretical fitting obtained with $\sigma_{23} = 1.0 \times 10^{-17} cm^2$, $\sigma_{45} = 4 \times 10^{-17} cm^2$ and $\tau_{isc} = 25\,ns$. A very small saturation for the first few pulses can be observed, which is related to the population buildup in level $|1\rangle$. After this initial step, level $|2\rangle$ starts to be populated, allowing a population transfer to the triplet state. Since this state has an absorption cross-section higher than that of level $|2\rangle$, a reverse saturation occurs. If the transition $e_g \rightarrow a_{2u}$ is not taken into account in the model, the plateau observed for the first few pulses does not appear.

5.2 (b) NLOA in the femtosecond regime

This section reports the resonant nonlinear absorption spectrum of Ytterbium Bisphthalocyanine (YbPc2) from 500 up to 675 nm in the femtoseconds regime determined through the WLC Z-scan. The results indicate the presence of SA, at the Q-band region, and a RSA, around 530 nm (De Boni et al., 2006). The line with circles in Figure 11 shows the nonlinear spectrum (transmittance change (ΔT) spectrum) of YbPc$_2$ obtained through the WLC Z-scan technique. Three distinct behaviors can clearly be observed: (i) a strong SA process that follows the Q-band, indicated by the positive ΔT values, (ii) an excited state absorption which gives an effective SA process below the Q-band and (iii) the negative ΔT values due to a RSA mechanism.

Due to the WLC-pulse chirp, the red portion of the pulse, which is resonant with the Q-band, promotes the population to the first excited state. In this case, a simplification of the diagram showed in Figure 10 can be used, which consists in considering only the first three levels (0, 1 and 2). From this assumption, the population dynamics is established to understand the experimental results. According to this consideration, molecules at the ground state $|0\rangle$ (a_{2u}) can be promoted to the first excite state $|1\rangle$ (e_g^*) by one-photon absorption (Q-Band; $a_{2u} \rightarrow e_g^*$), being subsequently excited to level $|2\rangle$. Molecules at level $|1\rangle$ decay radiatively to the ground state with a relaxation time $\tau_{10} = 4$ ns, which is much longer than the WLC-pulse duration. The upper excited singlet level, $|2\rangle$, is assumed to be too short-lived to present any significant population buildup. In this case, molecules are accumulated in the first excited state and the absorption cross-section between the states $|1\rangle$

and $|2\rangle$ can be determined. As the intersystem-crossing time for this molecule is around 25 ns, no triplet states need to be considered for the temporal regime of the pulses employed. The rate equations used to describe the fraction of molecules, n_i, at each level are obtained from Eq. (12-15) but considering only terms related to levels 0, 1 and 2. The time evolution of the nonlinear absorption can be calculated according to:

$$\alpha(\lambda, t) = N[n_0(t)\sigma_{01}(\lambda) + n_1(t)\sigma_{12}(\lambda)] \tag{17}$$

where N is the sample concentration. When $\sigma_{01} > \sigma_{12}$, the sample presents a decrease in the effective absorption as the excited state is populated (SA). On the other hand, if $\sigma_{01} < \sigma_{12}$, the sample becomes more opaque, characterizing a RSA process. The occurrence of SA or RSA depends on the contribution of different electronic states, excitation wavelength and pulse width. For the Q-band region (660 nm for instance), the model gives a σ_{12} of approximately zero, which leads to a SA that follows the absorption band, due to the population accumulated in the first excited state. Right below the Q-band (600 nm), SA does not follow the linear absorption. At 600 nm, for example, the theoretical fitting was obtained with σ_{12} = 0.5x10^{-18} cm^2, which is smaller than σ_{01} (SA). Around 530 nm, RSA was observed with σ_{12} = 10x10^{-18} cm^2, which is about four times higher than σ_{01}. A similar behavior in six distinct wavelengths was observed by Unnikrishnan e*t al.* (Unnikrishnan et al., 2002), even though they used much longer pulses (nanoseconds). Furthermore, due to the ultrashort pulses regime employed here, no triplet state is being populated and only the singlet state contributes to the observed RSA. The excited state absorption cross-section at 530 nm determined here ($\sigma_{12}/\sigma_{01} \approx 4$) is in agreement with a previous one obtained at 532 nm using the Z-scan technique with picosecond pulses (Mendonça et al., 2000,Mendonça et al., 2001, Misoguti et al., 1999). In that work, RSA was found to be related to singlet and triplet
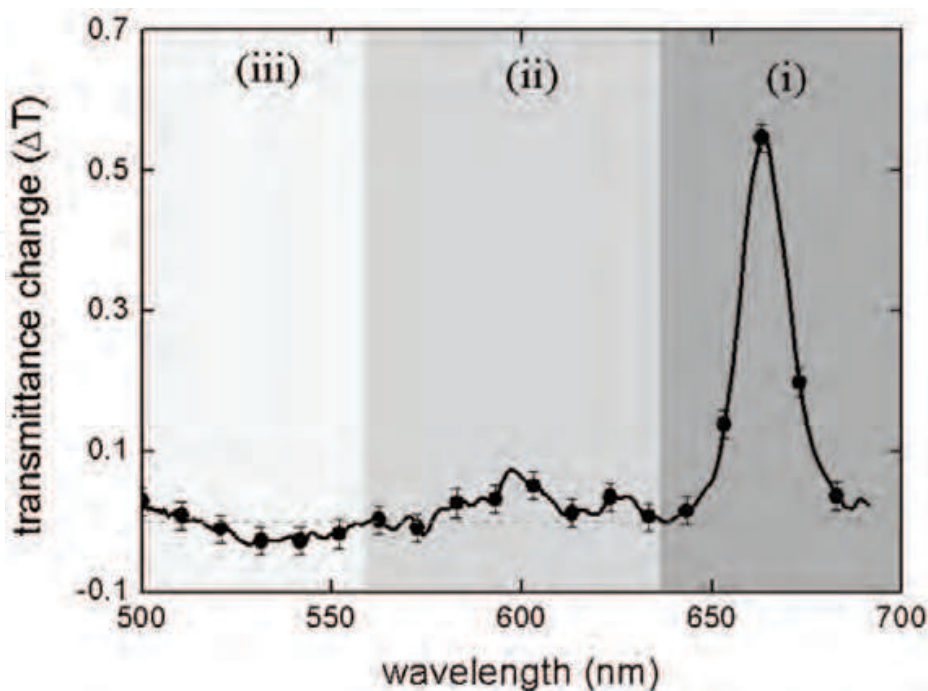

Fig. 11. Normalized transmittance change of YbPc$_2$ solution obtained with WLC Z-scan.

states, being mainly due to the last one, whose cross-section was found to be sixteen times higher than that of the ground state. The smaller singlet state contribution to RSA was comparable to the one presented here.

5.3 Indocyanine Green
5.3.1 NLOA in the nano and picosecond regime

The organic dye Indocyanine Green (ICG) presents high nonlinear optical properties, such as an efficient RSA (O'Flaherty et al., 2003), which makes it an interesting candidate for optics-related applications, such as optical limiting devices. Indocyanine Green can also be used as laser dye and saturable absorber. In medicine, ICG has been used for diagnosis and photo-dynamic therapy (PDT) of cancer. The intersystem-crossing time and quantum yield of triplet formation of ICG in different solvents have already been investigated (Reindl et al., 1997). These results revealed that the conversion efficiency to the triplet state is diminished by increasing the solvent polarity. The same behavior was observed for τ_{01}. For instance, in DMSO (apolar solvent), τ_{01} is 30 times greater than that observed in polar solvents. This section presents the nonlinear absorption of ICG obtained using single pulse and pulse train Z-scan techniques, both at 532 nm. Using the single pulse Z-scan and a theoretical analysis employing a three-energy level diagram, the excited singlet absorption cross-section was determined. Additionally, with the PTZ-scan technique and a five-energy level diagram, the intersystem-crossing time and the triplet absorption cross-section were obtained (De Boni et al.,2007).

Figure 12 shows the linear absorption spectrum of ICG diluted in DMSO. It has a strong band around 800 nm, related to the $\pi \rightarrow \pi*$ transition. At 532 nm, wavelength employed in the nonlinear optical measurements, only a small absorption was measured.
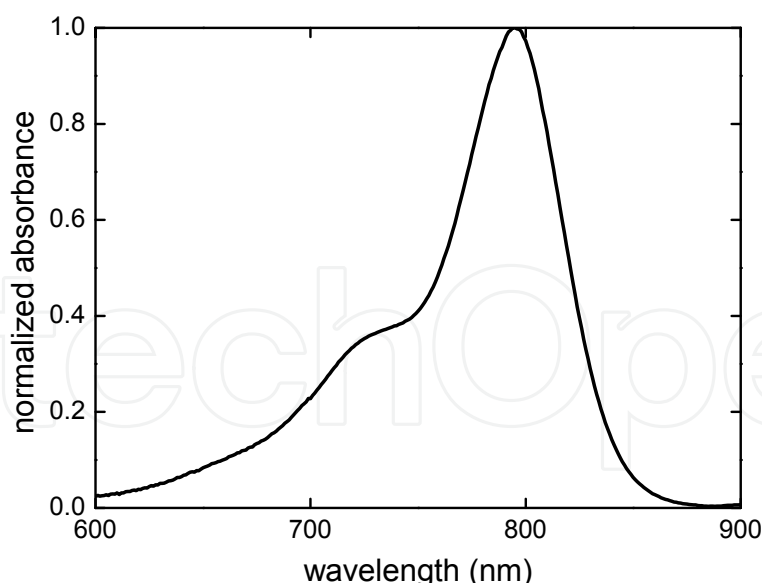

Fig. 12. Absorption spectrum of Indocyanine Green in DMSO.

Figure 13 (a) shows the decrease of the normalized transmittance (NT) for ICG as a function of the pulse irradiance, characterizing a RSA process. From this figure, it is possible to see saturation of the NT due to the accumulation of molecules in the first singlet excited state ($|1\rangle$) and to the depletion of the ground state ($|0\rangle$).
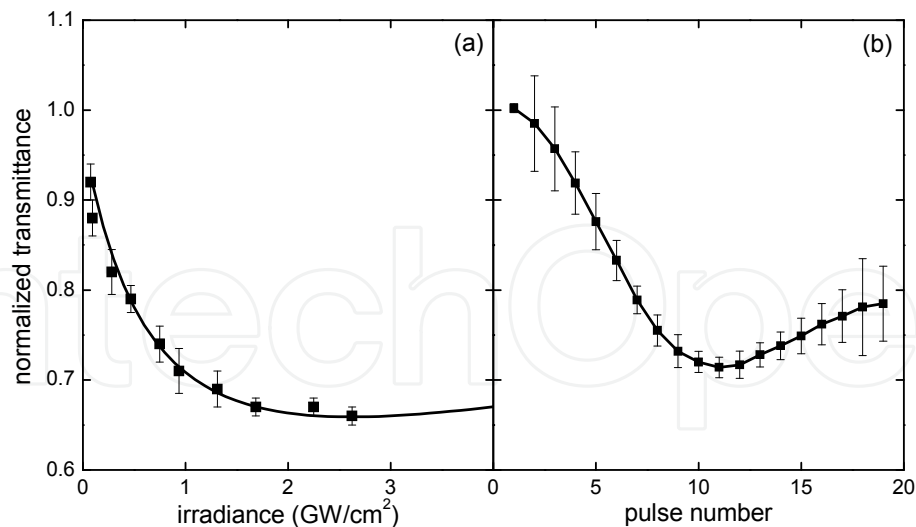
Fig. 13. (a) Normalized transmittance as a function of pulse irradiance for ICG in DMSO.
The solid line represents the fitting obtained with three-energy-level diagram.
(b) Normalized transmittance along of the Q-switch envelope (pulse number) for the same
sample. The solid line represents the theoretical curve obtained with parameters given in the
text, using the five-energy-level diagram.

As seen in Figure 13 (a), the saturation for ICG in DMSO occurs at ~ 2 GW/cm², a relatively
low intensity for this type of nonlinear process. This low saturation intensity for ICG is
related to its $|1\rangle \rightarrow |0\rangle$ transition lifetime (τ_{10} ~ 700 ps)(Reindl et al., 1997), which allows a
considerable accumulation of ICG molecules in the singlet excited state $|1\rangle$. With more
molecules in the first excited state, more transitions occur to the second excited state $|2\rangle$,
which presents an absorption cross-section approximately null. This process can be
visualized by the increase in the NT curve fitting that occurs after 3 GW/cm². In order to fit
the experimental data obtained with the single pulse Z-scan technique (Figure 13 (a)), the
three-energy-level diagram shown in Figure 14 (a), representing only the singlet states of the
molecule, was employed. As the band gap of ICG is around 1.5 eV, the internal conversion
(IC) process must be taken into account in the rate equations used to describe the population
dynamics. The triplet states were neglected because the duration of each single pulse is
shorter than the intersystem-crossing time. In this case, only the singlet states contribute to
the nonlinear absorption process. The transition lifetime (τ_{10}) can be described by
$1/\tau_{10} = /1/\tau_r + 1/\tau_{IC}$, where $\tau_r \approx 5$ ns and $\tau_{ic} \approx 840$ ps (Reindl et al., 1997) are singlet radiative
lifetime and internal conversion time respectively.
It was also assumed that the lifetime of the second excited singlet state, τ_{21}, is in the order of
a few femtoseconds; therefore, the population of this state is small at low irradiances. Hence,
to describe the fraction of molecules in each state, the rate equations used are given by:

$$\frac{dn_0}{dt} = -w_{01}n_0 + \frac{n_1}{\tau_{10}} \tag{18}$$

$$\frac{dn_1}{dt} = +w_{01}n_0 - w_{12}n_1 - \frac{n_1}{\tau_{10}} + \frac{n_2}{\tau_{21}} \tag{19}$$

$$\frac{dn_2}{dt} = +w_{12}n_1 - \frac{n_2}{\tau_{21}} \tag{20}$$

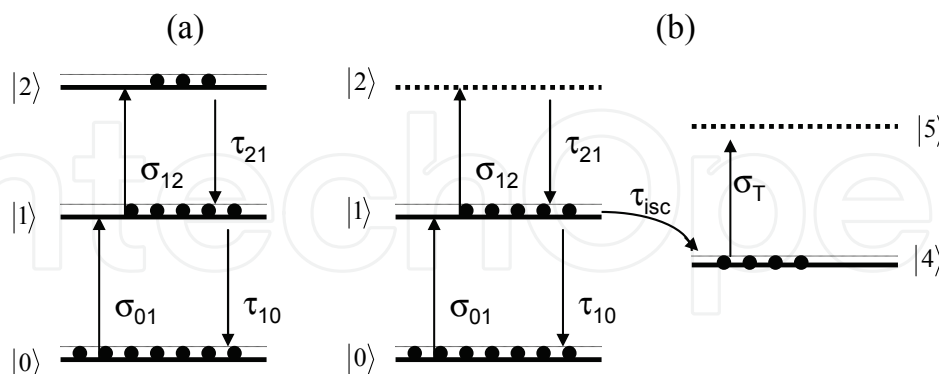(a)   (b)

Fig. 14. Three- (a) and five- (b) energy-level diagrams used to model the single pulse and pulse train Z-scan results for ICG.

where n_i's are the population fractions of the singlet states with $n_0 + n_1 + n_2 = 1$. The terms in these equations have already been described in the previous sections. The time dependence of absorption coefficient during the excitation is given by:

$$\alpha(t) = N\{n_0(t)\sigma_{01} + n_1(t)\sigma_{02}\} \tag{21}$$

As mentioned in the previous sections, α_{01} is obtained from the linear absorption spectrum ($\sigma_{01} = \alpha_{01}N$) and, therefore, the only adjustable parameter in this fitting procedure is σ_{12}. The value determined from the fitting was $\sigma_{12} = (12 \pm 1) \times 10^{-17} cm^2$, which is 75 times higher than the ground state cross-section ($\sigma_{01} = 0.16 \times 10^{-17} cm^2$).

Figure 13 (b) displays the accumulative nonlinearity for ICG obtained with pulse trains Z-scan technique. As seen, NT decreases with the pulse number up to about pulse 10, after which a small increase can be observed. This behavior could be understood by using a five-energy-level diagram, shown in Figure 14 (b). When excited by a pulse of the train to level $|1\rangle$, the molecule can undergo an intersystem-crossing to the triplet state $|4\rangle$, return to the ground state $|0\rangle$, or be promoted to a second excited state $|2\rangle$. With the arrival of the next pulse of the envelope, accumulative contributions to the optical nonlinearity, due to population built up in the long-lived (~ μs) $|4\rangle$ state, start to appear. The molecules in this state can be promoted to a second triplet state, $|5\rangle$, resulting in a change in the molecule absorption. Given the low irradiance of each individual pulse of the train and the short lifetime of levels $|2\rangle$ and $|5\rangle$, their population can be neglected. Considering this model, the fractions of molecules in each state are given by:

$$\frac{dn_0}{dt} = -w_{01}n_0 + \frac{n_1}{\tau_{10}} \tag{22}$$

$$\frac{dn_1}{dt} = +w_{01}n_{01} - \frac{n_1}{\tau_f} \tag{23}$$

$$\frac{dn_4}{dt} = \frac{n_1}{\tau_{isc}} \tag{24}$$

in which n_4 is the population fraction of the first triplet state. The $|1\rangle \rightarrow |0\rangle$ transition lifetime is given by $1/\tau_{01} = 1/\tau_f - 1/\tau_{isc}$, where τ_f and τ_{isc} are the fluorescence lifetime and the intersystem-crossing time respectively. This set of equations was numerically solved, yielding the time evolution of the absorption as:

$$\alpha(t) = N\{n_0(t)\sigma_{01} + n_1(t)\sigma_{12} + n_4(t)\sigma_T\} \tag{25}$$

where σ_T is the triplet state transition absorption cross-section. The only adjustable parameters are σ_T and τ_{isc}, once σ_{01} and σ_{12} are already known from the single pulse Z-scan analysis. The solid line in Figure 13(b) represents the best fitting obtained.

The intersystem-crossing time obtained through the fitting was $\tau_{isc} \approx (4\pm1)ns$, which is in good agreement with the one reported in the literature (Reindl et al., 1997). The quantum yield of triplet formation, ϕ_T, was calculated using $\phi_T = \tau_f / \tau_{isc}$ and τ_{isc} values, providing $\phi_T \approx 15\%$. The absorption cross-section of the triplet state found through the fitting procedure was $\sigma_T = (5\pm1)\times10^{-17} cm^2$. This value is 31 times higher than that of the ground state cross-section ($\sigma_T = 0.16\times10^{-17} cm^2$). It was observed that σ_{12} is higher than σ_T ($\sigma_{12}/\sigma_T \approx 2.4$), indicating that the excited singlet state gives a higher contribution to the RSA process for ICG. In table 1 are the spectroscopic parameters obtained by fitting single and pulse train Z-scan data. This table also shows other ICG spectroscopic parameters obtained from the literature.

σ_{01}	σ_{12}	σ_T	τ_f	ϕ_{fl}	ϕ_T	ϕ_{ic}	k_{isc}	k_r	k_{ic}
0.16	12 ± 1	5 ± 0.5	580 ± 40	0.106	0.15 ± 0.04	0.74 ± 0.05	2.5 ± 0.6	1.82 ± 0.07	11 ± 1

Table 1. Cross-section values (x10^{-17} cm^2) for ground (σ_{01}), excited singlet (σ_{12}) and excited triplet (σ_T) states at 532 nm. Fluorescence lifetime (τ_f) (ps) (Reindl et al., 1997), fluorescence (ϕ_{fl}) (Reindl et al., 1997), triplet (ϕ_T) and internal conversion (ϕ_{ic}) quantum yields and rates constants (x10^8 s^{-1}) of intersystem-crossing (k_{isc}), radiative (k_r) (Reindl et al., 1997) and internal conversion (k_{ic}) of ICG/DMSO solution.

5.4 Cytochrome C
5.4.1 NLOA in the nano and picosecond regime

Cytochrome C (cyt c) is one of the most intensively investigated redox proteins, which act as electron carriers in the respiratory chain. It contains a covalent heme group linked to polypeptide chains, which prevent aggregation, feature desirable, for instance, in Photodynamic therapy (PDT). The heme group is an iron porphyrin, the same that is found in hematoporphyrins, with peripheral groups bonded to pyrrole rings, while the polypeptide chains are polymers made by amino acid residues linked by peptide bonds. This section presents some results of Z-scan technique employed to characterize the spectroscopic parameters and the dynamics of excited states of Fe^{3+} cyt c molecules, combined to pump-probe (Shapiro, 1977) measurements at 532 nm. The results clearly show that the nonlinearity origin can be ascribed to population effects of the Q-band followed by

a fast relaxation back to the singlet ground state. The saturable absorption process observed has an intensity dependence and time evolution that can be described with a three-energy-level diagram, yielding the excited state parameters of cyt c (Neto et al., 2004).

Figure 15 shows the UV-Vis absorption spectrum for oxidized cyt c water solution. The strong band at 400 nm corresponds to the B (Soret) band, while the transition around 530 nm is attributed to the Q-band of the metalloporphyrin complex. The origin of these bands is related to π-π* and charge transfer transitions. According to the absorption spectrum, only the Q-band is excited when light at 532 nm is used.
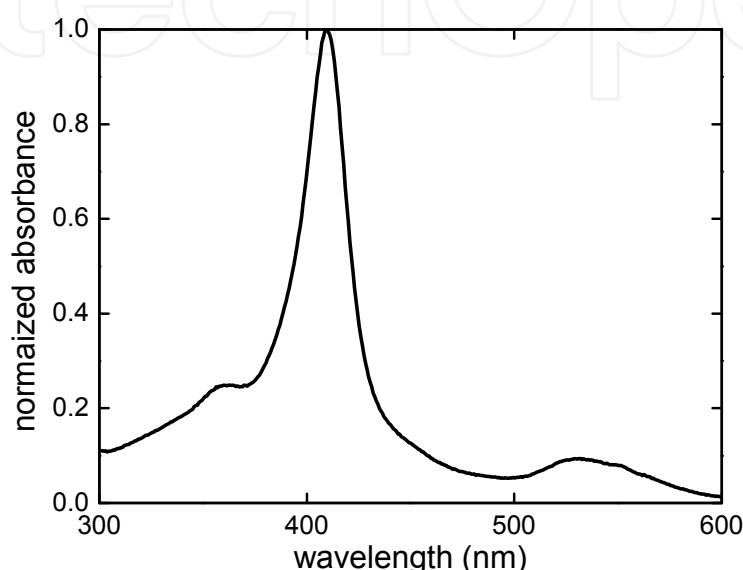

Fig. 15. Normalized absorbance spectrum of oxidized cyt c in water solution.

The results of the Z-scan measurements as a function of the pulse irradiance, in distinct temporal regimes (ps and fs), are depicted as solid circles in Figure 16 (a) and (b). To explain the behavior observed, the three-energy-level diagram presented in the inset of Figure 16 was considered, assuming that only the singlet states contribute to the nonlinear absorption process. This assumption is based on the fact that the pulse duration is faster than the intersystem-crossing time, which avoids any appreciable triplet state population buildup during the light-matter interaction time. In addition, the excited singlet state $|2\rangle$ was assumed to be too short-lived to present an appreciable population buildup.

According to the three-energy-level diagram proposed, molecules at the ground state $|0\rangle$ can be promoted to level $|1\rangle$ when excited by laser pulses of 70 ps at 532 nm, then decaying back to $|0\rangle$ with a relaxation time τ_{10}. Two-photon absorption processes were neglected because, under resonant conditions, excited state processes (saturable absorption) prevail. (Andrade et al., 2004). The rate equations used to describe the fraction of molecules remaining at ground state are:

$$\frac{dn_0}{dt} = -W_{01}n_0 + \frac{1-n_0}{\tau_{10}} \qquad (25)$$

where n_0 and n_1 are the population fractions of the ground and first excited singlet state respectively and $W_{01} = \sigma_{01}I/h\nu$ is the one-photon transition rate. All the terms in Eq. 25
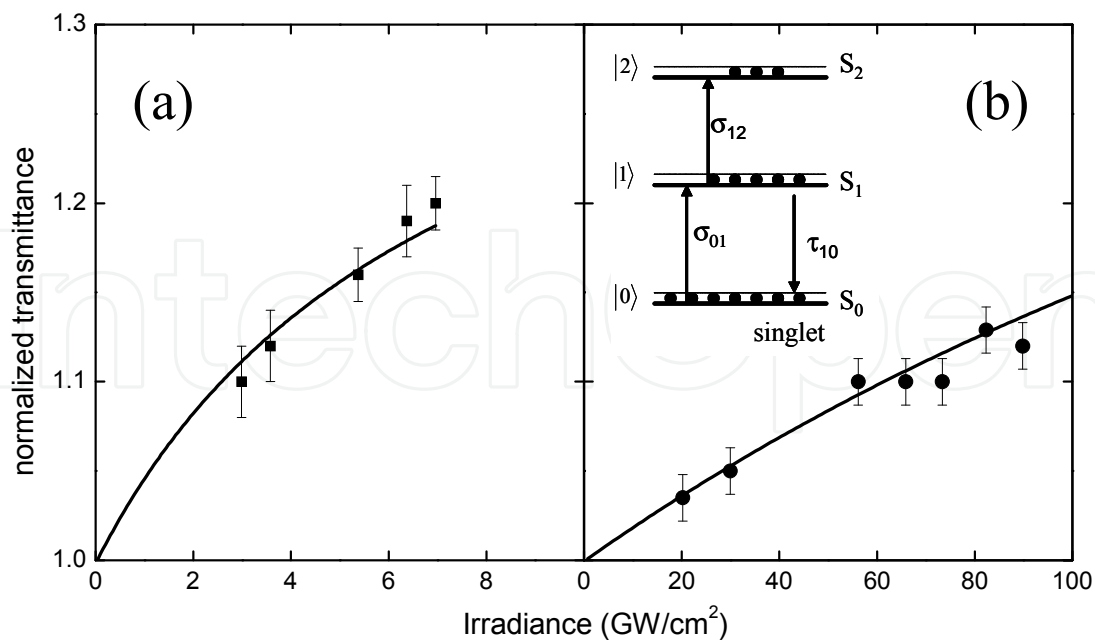
Fig. 16. (a) Normalized transmittance as a function of the 70 ps pulse irradiance at 532 nm. (b) Normalized transmittance as a function of the 120 fs pulse irradiance at 530 nm. The solid line in (a) and (b) are the fitting obtained with the three-energy-level model (inset) with the parameters given in the text.

have already been defined. $n_0 + n_1 = 1$, because the population of the $|2\rangle$ state is neglected. σ_{01} was determined as 4.1×10^{-17} cm².

In addition, an independent measurement was performed to determine the decay time of level $|1\rangle$, τ_{10}, with the degenerate pump-probe technique at 532 nm, yielding a characteristic time of 2.7 ps (Neto et al., 2004). Therefore, since all parameters of Eq. (25) are determined, it can be numerically solved using a Gaussian temporal intensity pattern for the laser pulse, yielding the population dynamics within the laser pulse. The time-dependent absorption coefficient in this case is:

$$\alpha(t) = N\{n_0(t)\sigma_{01} + n_1(t)\sigma_{12}\} \tag{26}$$

where N is the concentration, σ_{12} is the excited state cross-section, and n_0 and n_1 are the population fraction in each state. By fitting the experimental data, the best value found for σ_{12} was 3.7×10^{-17} cm², which is on the same order of magnitude of those reported in the literature for metallporphyrins (Blau et al., 1985, Neto et al., 2003). Since the intersystem-crossing time is unknown, the possibility of the triplet state acquiring some population cannot be disregarded *a priori*. In order to confirm the excited singlet state cross-section value and the three-energy-level model assumed, Z-scan measurements using 120 fs pulses at 532 nm were carried out. In this case, one can safely state that the pulse duration is faster than the intersystem-crossing time and that there is no triplet state population during the pulse interaction, which certainly allows the use of the three-energy-level diagram. Again, an increase due to a saturable absorption mechanism is observed in the normalized transmittance as a function of irradiance, displayed in Fig 16(b), indicating that laser pulses are populating the excited state. The solid line represents the theoretical fitting obtained

with the model described previously, resulting in σ_{12} = 3.7 x 10^{-17} cm^2, which is the same value found in the picosecond Z-scan experiment. This result indicates that, even when picosecond pulses are used, the triplet state is not populated, supporting the assumption made on the three-level energy model used to explain the experimental results. It also implies that the intersystem-crossing time of cyt c should be in the order of a few hundred picoseconds (Sazanovich et al., 2003).

The short singlet state lifetime is a clear indication of the fast intersystem-crossing time, which is a characteristic of porphyrins with open shell ions (Kalyanasundaram, 1992). This short intersystem-crossing time, compared with those of closed shell porphyrins (Kalyanasundaram, 1984), indicates an efficient singlet-triplet conversion, making hematoporphyrins suitable for applications as a PDT sensitizer. Besides, cyt c is a biocompatible molecule, which is a requirement for medical applications.

6. Conclusion

This chapter aimed to describe the resonant nonlinear optical properties of four important organic molecules: Chlorophyll A, Indocyanine Green, Ytterbium Bisphthalocyanine and Cytochrome C, which are materials that present interesting optical nonlinearities for applications in optical devices. It was shown that Chlorophyll A solution exhibits a RSA process for Q-switched and mode-locked laser pulses, with an intersystem-crossing time relatively fast and a triplet state cross section value twice higher than that of the singlet. Such features are desired for applications in PDT. However, due to the low triplet–singlet cross-section ratio, Chlorophyll A is not expected to be efficient as an optical limiter. In addition, the excited state population buildup generated with the WLC Z-scan technique can be advantageously used to shape the pulse intensity spectrum in order to match the most intense linear absorption band of the material. As a consequence, one can obtain an enhancement of the nonlinear absorption in a transparent region through excited state absorption. In practical terms, WLC pulses could be used in applications where a high RSA process is needed in the blue region of the spectrum. RSA at 532 nm for ICG solution was also described. For single pulse experiments, it was determined that the excited singlet state cross-section is 75 times higher than that of the ground state. However, when pulse trains are employed, triplet population is identified, with an intersystem-crossing time in the nanosecond time scale. In this case, the triplet absorption cross-section found is 31 times higher than the ground state one. These results indicate ICG as a candidate for applications requiring high RSA, such as optical limiters and all-optical switches. Regarding Ytterbium Bis-phtalocyanine, it was shown that this molecule presents two possible ground state levels and both can absorb the excitation light for some wavelength range. When using femtosecond laser pulses, it was also possible to observe distinct resonant nonlinear absorption behaviours (SA and RSA) depending on the wavelength. Basically, the excited state absorption cross-section is approximately zero in the Q-band region, giving origin to a strong SA process. Oxidized Cytochrome C in water solution exhibits a saturable absorption process when resonant excitation at 532 nm (Q-band) is employed. Its short singlet state lifetime indicates a relatively fast intersystem-crossing time that can lead to an efficient formation of the triplet state. Such feature prompts this molecule as an efficient sensitizer for PDT applications. Therefore, organic molecules presenting high nonlinear optical absorption processes are potential candidates as active media for applications in optical devices.
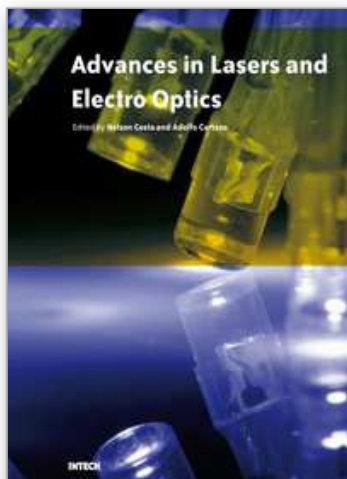
7. Acknowledgment

8. References

Andrade, A. A.; Neto, N. M. B.; Misoguti, L.; De Boni, L.; Zilio, S. C. & Mendonca, C. R. (2004). Two-photon absorption investigation in reduced and oxidized cytochrome c solutions. *Chemical Physics Letters*, 390, 4-6(Jun 1):506-510.

Baker, N. R. & Rosenqvist, E. (2004). Applications of chlorophyll fluorescence can improve crop production strategies: an examination of future possibilities. *Journal of Experimental Botany*, 55, 403(Aug):1607-1621.

Balu, M.; Hales, J.; Hagan, D. J. & Van Stryland, E. W. (2004). White-light continuum Z-scan technique for nonlinear materials characterization. *Optics Express*, 12, 16(Aug 9):3820-3826.

Banfi, G.; Degiorgio, V. & Ricard, D. (1998). Nonlinear optical properties of semiconductor nanocrystals. *Advances in Physics*, 47, 3(May-Jun):447-510.

Bhawalkar, J. D.; He, G. S. & Prasad, P. N. (1996). Nonlinear multiphoton processes in organic and polymeric materials. *Reports on Progress in Physics*, 59, 9(Sep):1041-1070.

Blau, W.; Byrne, H.; Dennis, W. M. & Kelly, J. M. (1985). Reverse Saturable Absorption in TetraPhenylPorphyrins. *Optics Communications*, 56, 1: 25-29.

Calvete, M.; Yang, G. Y. & Hanack, M. (2004). Porphyrins and phthalocyanines as materials for optical limiting. *Synthetic Metals*, 141, 3(Mar 25):231-243.

Carter, G. A. & Spiering, B. A. (2002). Optical properties of intact leaves for estimating chlorophyll concentration. *Journal of Environmental Quality*, 31, 5(Sep-Oct):1424-1432.

Correa, D. S.; De Boni, L.; dos Santos, D. S.; Neto, N. M. B.; Oliveira, O. N.; Misoguti, L.; Zilio, S. C. & Mendonca, C. R. (2002). Reverse saturable absorption in chlorophyll A solutions. *Applied Physics B-Lasers and Optics*, 74, 6(Apr):559-561.

De Boni, L.; Andrade, A. A.; Misoguti, L.; Mendonca, C. R. & Zilio, S. C. (2004). Z-scan measurements using femtosecond continuum generation. *Optics Express*, 12, 17(Aug 23):3921-3927.

De Boni, L.; Correa, D. S.; Pavinatto, F. J.; dos Santos, D. S. & Mendonca, C. R. (2007). Excited state absorption spectrum of chlorophyll a obtained with white-light continuum. *Journal of Chemical Physics*, 126, 16(Apr 28):165102.

De Boni, L.; Gaffo, L.; Misoguti, L. & Mendonca, C. R. (2006). Nonlinear absorption spectrum of ytterbium bis-phthalocyanine solution measured by white-light continuum Z-scan technique. *Chemical Physics Letters*, 419, 4-6(Feb 26):417-420.

De Boni, L.; Rezende, D. C. J. & Mendonca, C. R. (2007). Reverse saturable absorption dynamics in indocyanine green. *Journal of Photochemistry and Photobiology a-Chemistry*, 190, 1(Jul 5):41-44.

Fisher, A. M. R.; Murphree, A. L. & Gomer, C. J. (1995). Clinical and Preclinical Photodynamic Therapy. *Lasers in Surgery and Medicine*, 17, 1:2-31.

Frackowiak, D.; Planner, A.; Waszkowiak, A.; Boguta, A.; Ion, R. M. & Wiktorowicz, K. (2001). Yield of intersystem (singlet-triplet) crossing in phthalocyanines evaluated

on the basis of a time in resolved photothermal method. *Journal of Photochemistry and Photobiology a-Chemistry*, 141, 2-3(Jul 2):101-108.

Gouterman, M. (1961). Spectra of Porphyrins. *Journal of Molecular Spectroscopy*, 6, 1:138-163.

Hasegawa, J.; Ozeki, Y.; Ohkawa, K.; Hada, M. & Nakatsuji, H. (1998). Theoretical study of the excited states of chlorin, bacteriochlorin, pheophytin a and chlorophyll a by the SAC/SAC-CI method. *Journal of Physical Chemistry B*, 102, 7(Feb 12):1320-1326.

He, G. S.; Tan, L. S.; Zheng, Q. & Prasad, P. N. (2008). Multiphoton absorbing materials: Molecular designs, characterizations, and applications. *Chemical Reviews*, 108, 4(Apr):1245-1330.

Kalyanasundaram, K. (1984). Photochemistry of water-soluble porphyrins: Comparative study of isomeric tetrapyridyl- and tetrakis (N - methylpyridiniumyl) porphyrins. *Inorganic Chemistry*, 23, 16, 2453-2459.

Kalyanasundaram, K. (1992). *Photochemistry of polypyridine and porphyrin complexes*, Academic PressSan Diego.

Linnanto, J. & Korppi-Tommola, J. (2000). Spectroscopic properties of Mg-chlorin, Mg-porphin and chlorophylls a, b, c(1), c(2), c(3) and d studied by semi-empirical and ab initio MO/CI methods. *Physical Chemistry Chemical Physics*, 2, 21:4962-4970.

Loppacher, C.; Guggisberg, M.; Pfeiffer, O.; Meyer, E.; Bammerlin, M.; Luthi, R.; Schlittler, R.; Gimzewski, J. K.; Tang, H. & Joachim, C. (2003). Direct determination of the energy required to operate a single molecule switch. *Physical Review Letters*, 90, 6(Feb 14):066107.

Mendonça, C. R.; Gaffo, L.; Misoguti, L.; Moreira, W. C.; Oliveira, O. N. & Zilio, S. C. (2000). Characterization of dynamic optical nonlinearities in ytterbium bis-phthalocyanine solution. *Chemical Physics Letters*, 323, 3-4(Jun 16):300-304.

Mendonça, C. R.; Gaffo, L.; Moreira, W. C.; Oliveira, O. N. & Zilio, S. C. (2001). Optical properties of ytterbium bis-phthalocyanine solution. *Synthetic Metals*, 121, 1-3(Mar 15):1477-1478.

Michel-Beyerle, M. E. (1985). *Antennas and Reaction Centers of Photosynthetic Bacteria*, Springer-VerlagBerlin.

Misoguti, L.; Mendonca, C. R. & Zilio, S. C. (1999). Characterization of dynamic optical nonlinearities with pulse trains. *Applied Physics Letters*, 74, 11(Mar 15):1531-1533.

Misoguti, L.; Mendonça, C. R. & Zilio, S. C. (1999). Characterization of dynamic optical nonlinearities with pulse trains. *Applied Physics Letters*, 74, 11: 1531-1533.

Neto, N. M. B.; Andrade, A. A.; De Boni, L.; Misoguti, L.; Zilio, S. C. & Mendonca, C. R. (2004). Excited-state absorption in oxidized cytochrome c solution. *Applied Physics B-Lasers and Optics*, 79, 6(Oct):751-754.

Neto, N. M. B.; Correa, D. S.; Dos Santos, D. S.; Misoguti, L.; Oliveira, O. N.; Zilio, S. C. & Mendonca, C. R. (2003). Influence of photodegradation on the optical limiting process of chlorophyll A. *Modern Physics Letters B*, 17, 2(Jan 30):83-87.

Neto, N. M. B.; De Boni, L.; Rodrigues, J. J.; Misoguti, L.; Mendonca, C. R.; Dinelli, L. R.; Batista, A. A. & Zilio, S. C. (2003). Dynamic saturable optical nonlinearities in free base tetrapyridylporphyrin. *Journal of Porphyrins and Phthalocyanines*, 7, 6:452-456.

Neto, N. M. B.; Oliveira, S. L.; Misoguti, L.; Mendonca, C. R.; Goncalves, P. J.; Borissevitch, I. E.; Dinelli, L. R.; Romualdo, L. L.; Batista, A. A. & Zilio, S. C. (2006). Singlet excited state absorption of porphyrin molecules for pico- and femtosecond optical limiting application. *Journal of Applied Physics*, 99, 12(Jun 15):123103.

O'Flaherty, S. M.; Hold, S. V.; Cook, M. J.; Torres, T.; Chen, Y.; Hanack, M. & Blau, W. J. (2003). Molecular engineering of peripherally and axially modified phthalocyanines for optical limiting and nonlinear optics. *Advanced Materials*, 15, 1(Jan 3):19-+.

Pang, Y.; Samoc, M. & Prasad, P. N. (1991). 3rd-Order Nonlinearity and 2-Photon-Induced Molecular-Dynamics - Femtosecond Time-Resolved Transient Absorption, Kerr Gate, and Degenerate 4-Wave-Mixing Studies in Poly(Para-Phenylene Vinylene) Sol-Gel Silica Film. *Journal of Chemical Physics*, 94, 8(Apr 15):5282-5290.

Parusel, A. B. J. & Grimme, S. (2000). A theoretical study of the excited states of chlorophyll a and pheophytin a. *Journal of Physical Chemistry B*, 104, 22(Jun 8):5395-5398.

Prasad, P. N. (1991). Polymeric Materials for Nonlinear Optics and Photonics. *Polymer*, 32, 10(1746-1751.

Prasad, P. N. & Willians, D. J. (1991). *Introduction to Nonlinear Optical Effects in Molecules and Polymers*, Wiley-InterscienceNew York.

Reindl, S.; Penzkofer, A.; Gong, S. H.; Landthaler, M.; Szeimies, R. M.; Abels, C. & Baumler, W. (1997). Quantum yield of triplet formation for indocyanine green. *Journal of Photochemistry and Photobiology a-Chemistry*, 105, 1(May 15):65-68.

Rivadossi, A.; Zucchelli, G.; Garlaschi, F. M. & Jennings, R. C. (2004). Light absorption by the chlorophyll a-b complexes of photosystem II in a leaf with special reference to LHCII. *Photochemistry and Photobiology*, 80, 3(Nov-Dec):492-498.

Sazanovich, I. V.; Ganzha, V. A.; Dzhagarov, B. M. & Chirvony, V. S. (2003). Dichroism of the triplet-triplet transient absorption of copper(II) porphyrins in liquid solution. New interpretation of the subnanosecond relaxation component'. *Chemical Physics Letters*, 382, 1-2(Nov 28):57-64.

Scheidt, W. R. & Reed, C. A. (1981). Spin-State Stereochemical Relationships in Iron Porphyrins - Implications for the Hemoproteins. *Chemical Reviews*, 81, 6:543-555.

Shank, C. V.; Ippen, E. P. & Teschke, O. (1977). Sub-Picosecond Relaxation of Large Organic-Molecules in Solution. *Chemical Physics Letters*, 45, 2:291-294.

Shapiro, S. L.,(1977), *Topics in Applied Physics*, New York.

Sheik-Bahae, M.; Said, A. A. & Van Stryland, E. W. (1989). High-Sensitivity, Single-Beam N2 Measurements. *Optics Letters*, 14, 17(Sep 1):955-957.

Shen, Y. R. (1984). *The Principles of Nonlinear Optics*, John Wiley,0471889989 New York.

Shirk, J. S.; Lindle, J. R.; Bartoli, F. J. & Boyle, M. E. (1992). 3rd-Order Optical Nonlinearities of Bis(Phthalocyanines). *Journal of Physical Chemistry*, 96, 14(Jul 9):5847-5852.

Sundholm, D. (1999). Density functional theory calculations of the visible spectrum of chlorophyll a. *Chemical Physics Letters*, 302, 5-6(Mar 26):480-484.

Unnikrishnan, K. P.; Thomas, J.; Nampoori, V. P. N. & Vallabhan, C. P. G. (2002). Wavelength dependence of nonlinear absorption in a bis-phthalocyanine studied using the Z-scan technique. *Applied Physics B-Lasers and Optics*, 75, 8(Dec):871-874.

Vernon, L. P. & Seely, G. R. (1996). *The Chlorophylls*, AcademicNew York.

Wehling, A. & Walla, P. J. (2005). Time-resolved two-photon spectroscopy of photosystem I determines hidden carotenoid dark-state dynamics. *Journal of Physical Chemistry B*, 109, 51(Dec 29):24510-24516.

Zigmantas, D.; Hiller, R. G.; Sundstrom, V. & Polivka, T. (2002). Carotenoid to chlorophyll energy transfer in the peridinin-chlorophyll-a-protein complex involves an intramolecular charge transfer state. *Proceedings of the National Academy of Sciences of the United States of America*, 99, 26(Dec 24):16760-16765.

Advances in Lasers and Electro Optics

Edited by Nelson Costa and Adolfo Cartaxo

Lasers and electro-optics is a field of research leading to constant breakthroughs. Indeed, tremendous advances have occurred in optical components and systems since the invention of laser in the late 50s, with applications in almost every imaginable field of science including control, astronomy, medicine, communications, measurements, etc. If we focus on lasers, for example, we find applications in quite different areas. We find lasers, for instance, in industry, emitting power level of several tens of kilowatts for welding and cutting; in medical applications, emitting power levels from few milliwatt to tens of Watt for various types of surgeries; and in optical fibre telecommunication systems, emitting power levels of the order of one milliwatt. This book is divided in four sections. The book presents several physical effects and properties of materials used in lasers and electro-optics in the first chapter and, in the three remaining chapters, applications of lasers and electro-optics in three different areas are presented.

How to reference

In order to correctly reference this scholarly work, feel free to copy and paste the following:

Leonardo De Boni, Daniel S. Correa and Cleber R. Mendonca (2010). Nonlinear Optical Absorption of Organic Molecules for Applications in Optical Devices, Advances in Lasers and Electro Optics, Nelson Costa and Adolfo Cartaxo (Ed.), ISBN: 978-953-307-088-9, InTech, Available from: http://www.intechopen.com/books/advances-in-lasers-and-electro-optics/nonlinear-optical-absorption-of-organic-molecules-for-applications-in-optical-devices

INTECH

open science | open minds